15. V. P. Tronov and A. K. Rozentsvaig, "Coalescence of the disperse phase of liquid emulsions under pressure in the turbulent regime," Zh. Prikl. Khim., 49, No. 1, 231-232 (1976).
16. A. K. Rozentsvaig and L. P. Pergushev, "Coalescence of concentrated finely dispersed emulsions with turbulent mixing," Inzh.-Fiz. Zh., 40, No. 6, 1013-1018 (1981).
17. S. Gnanasundaram, T. E. Degaleeson, and G. S. Laddha, "Prediction of mean drop size in bath agitated vessels," Can. J. Chem. Eng., 57, No. 2, 141-144 (1979).
18. J. A. Cendel, A. A. Farugul, J. W. Finnigan, C. H. Wright, and J. G. Knudsen, "Laminar and turbulent flow of unstable liquid–liquid emulsions," AIChE J., 8, No. 3, 335-339 (1962).

LAMINAR FLOW OF AN INCOMPRESSIBLE FLUID IN A PLANE CHANNEL WITH UNIFORM UNIDIRECTIONAL INJECTION

B. Yu. Bakhvalov, V. M. Eroshenko, L. I. Zaichik, and A. A. Klimov

UDC 532.526

An experimental and theoretical study is made of flow hydrodynamics in a plane channel with a permeable wall.

Problems on gas flow in channels with permeable walls arise in connection with the study of heat and mass transfer processes in heat pipes, in the pore cooling of gas-turbine blades, and in several other important practical applications. The hydrodynamics of a developed flow in a plane channel were examined in [1-5], while flow in the initial section of a channel with symmetrical two-sided injection through the walls was investigated in [6, 7]. The hydrodynamics of a flow in a long narrow channel with one-sided injection were studied in [8]. The present work obtains numerical solutions of motion equations and experimentally studies nonsymmetrical flow in a plane channel with one permeable wall.

The motion equations, describing two-dimensional flow in an approximation of the boundary-layer theory, have the following form in dimensionless variables:

$$\frac{\partial \bar{u}_x}{\partial \bar{x}} + \frac{\partial \bar{u}_y}{\partial \bar{y}} = 0, \tag{1}$$

$$\bar{u}_x \frac{\partial \bar{u}_x}{\partial \bar{x}} + \bar{u}_y \frac{\partial \bar{u}_x}{\partial \bar{y}} = -\frac{d\bar{p}}{d\bar{x}} + \frac{\partial^2 \bar{u}_x}{\partial \bar{y}^2}. \tag{2}$$

With a uniform velocity profile at the inlet section of the channel, the boundary conditions for Eqs. (1) and (2) will be

$$\bar{x} = 0 \quad \bar{u}_x = 1; \quad \bar{y} = 0 \quad \bar{u}_x = 0, \quad \bar{u}_y = \mathrm{Re}_Y; \quad \bar{y} = 1 \quad \bar{u}_x = \bar{u}_y = 0. \tag{3}$$

Figures 1 and 2 show results of numerical solution of systems (1) and (2), with boundary conditions (3), for different values of the parameter Re_Y. Figure 1 shows profiles of the axial velocity component, normalized by the mean velocity in the cross section of interest $U = U_0(1 + \mathrm{Re}_Y\bar{x})$, for $\mathrm{Re}_Y = 80$. The velocity distribution is clearly S-shaped in the initial section of the channel (curves 2 and 3 in Fig. 1), which is typical of flow in a boundary layer with injection [9]. As $\bar{x}$ increases, the point of inflection of the velocity profile becomes less distinct and the velocity distribution approaches the developed profile found from similarity solution of the motion equations. An increase in injection rate is accompanied by a shift in the velocity maximum toward the impermeable wall, and the distribution of u_x approaches the limitingdistribution $u_x = U \sin(\pi\bar{y}/2)$ [5]. Father from the channel inlet, the calculated velocity profiles agree with those measured in [8].

G. M. Krzhizhanskii Energy Institute, Moscow. Translated from Inzhenerno-Fizicheskii Zhurnal, Vol. 42, No. 3, pp. 372-376, March, 1982. Original article submitted February 17, 1981.

0022-0841/82/4203-0259$07.50

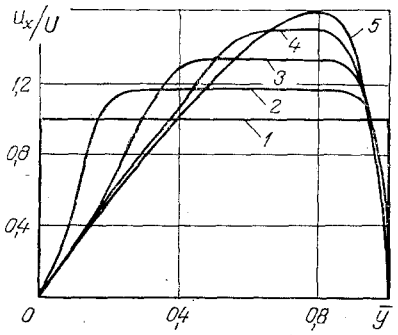

Fig. 1

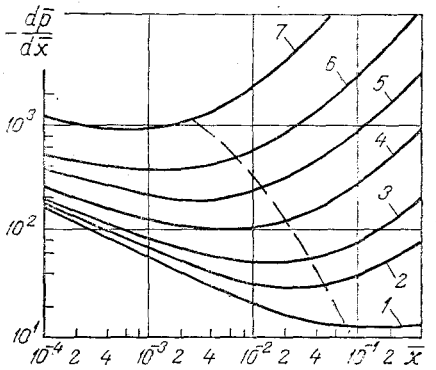

Fig. 2

Fig. 1. Profiles of longitudinal velocity at different channel cross sections: 1) $\bar{x} = 0$; 2) $5 \cdot 10^{-4}$; 3) $2 \cdot 10^{-3}$; 4) $6 \cdot 10^{-3}$; 5) ∞.

Fig. 2. Change in pressure gradient along channel: 1 — Re_V = 0; 2 — 5; 3 — 10; 4 — 25; 5 — 50; 6 — 100; 7 — 250.

Analysis of the velocity distributions obtained shows that, with vigorous injection ($Re_V \gg 1$) a certain distance from the inlet section, the velocity gradient at the permeable wall, referred to the local mean velocity U, practically ceases to be dependent on the longitudinal coordinate $\bar{x}$ and the Reynolds number associated with the injection Re_V. This situation can be explained by the fact that, in the case of vigorous injection, viscous forces in the boundary region can be ignored compared to inertial forces. Thus, allowing for boundary conditions (3), it follows from Eq. (2) that

$$\left(\frac{\partial \bar{u}_x}{\partial \bar{y}}\right)_{\bar{y}=0} = -\frac{1}{\mathrm{Re}_V}\frac{d\bar{p}}{d\bar{x}}. \tag{4}$$

The longitudinal pressure gradient can be determined from the unidimensional momentum conservation equation obtained by integrating (2) over the channel cross section:

$$-\frac{d\bar{p}}{d\bar{x}} = \frac{d(\beta \bar{U}^2)}{d\bar{x}} + \left(\frac{\partial \bar{u}_x}{\partial \bar{y}}\right)_{\bar{y}=0} - \left(\frac{\partial \bar{u}_x}{\partial \bar{y}}\right)_{\bar{y}=1}. \tag{5}$$

The value of the momentum flux coefficient β, characterizing the degree of deviation of the axial-velocity profile from uniformity, ranges within 1.00-1.24 under the conditions being examined. The derivatives of velocity at the permeable and nonpermeable walls have the following orders at $Re_V \gg 1$:

$$\left(\frac{\partial u_x/U}{\partial \bar{y}}\right)_{\bar{y}=0} = O(1), \quad -\left(\frac{\partial u_x/U}{\partial \bar{y}}\right)_{\bar{y}=1} = O(\mathrm{Re}_V^{1/2}).$$

Ignoring the change in β over the channel length, we have the following, accurate to within $O(Re_V^{1/2})$, from (5):

$$-\frac{d\bar{p}}{d\bar{x}} = 2\beta \bar{U}\frac{d\bar{U}}{d\bar{x}} = 2\beta\,\mathrm{Re}_V. \tag{6}$$

From Eqs. (4) and (6) we obtain

$$\left(\frac{\partial u_x/U}{\partial \bar{y}}\right)_{\bar{y}=0} = 2\beta.$$

Thus, with vigorous injection, the relative-velocity gradient at the permeable wall is actually slightly dependent on the flow parameters. This is particularly evident from Fig. 1.

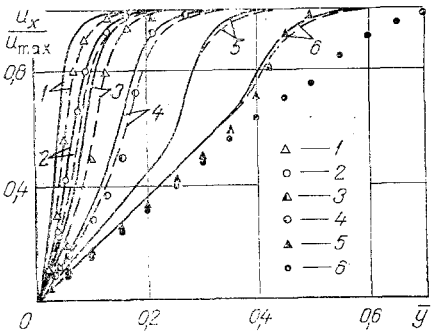

Fig. 3. Comparison of measured and calculated longitudinal-velocity distributions: 1 — Re_γ = 25, x/h = 1.25; 2 — 25 and 3; 3 — 100 and 1.25; 4 — 100 and 3; 5 — 550 and 1.25; 6 — 550 and 3.

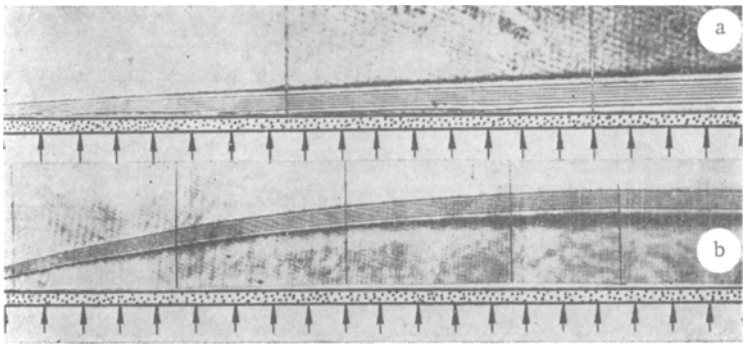

Fig. 4. Flow interferograms with the injection of carbon dioxide into an air flow: a) Re_γ = 30; b) 300.

The pressure drop increases with an increase in injection rate, since some of the energy of the flow must be spent on accelerating the fluid injected into the channel. The dependence of the pressure gradient on the longitudinal coordinate is nonmonotonic (Fig. 2). As in the case of the absence of injection, the drop in $|d\bar{p}/d\bar{x}|$ is explained by a reduction in friction on the walls with the restructuring of the velocity profile from uniform to developed. The increase in $|d\bar{p}/d\bar{x}|$ is connected with acceleration of the flow under the influence of the injected liquid, the effect of which begins at a certain distance from the inlet to predominate over the reduction in surface friction. The value of $(1/\overline{U})(d\bar{p}/d\bar{x})$ is independent of $\bar{x}$ in the region of developed flow; on this basis, we defined the length of the inlet section as the distance over which $(1/\overline{U})(d\bar{p}/d\bar{x})$ differs by 1% from the corresponding value for a fully developed flow (the dashed line in Fig. 2). As in the case of two-sided injection [6, 7], the length of the inlet section decreases markedly with an increase in Re_γ.

Figure 3 shows the distribution of the longitudinal velocity component measured with the injection of nitrogen into an air flow and normalized by the value of the maximum velocity in the section of interest. The experiments were conducted on a gasdynamic unit equipped with a Max—Sender interferometer [10]. The velocity distribution was measured with a hot-wire anemometer. The floor of the channel, 40 × 40 mm in cross section, was made of a porous material and was 132 mm long. The side walls were made of optical glass. Carbon dioxide was injected through the permeable surface to visualize the current in the air flow. Figure 4 presents inteferograms depicting the flow pattern in lines of equal concentration for moderate and vigorous injections and making it possible to distinguish characteristic zones in the region of interaction of the main flow and injected flow.

With moderate injection rates (Fig. 4a), the zone in which the incoming and injected gases are mixed is not pushed away from the wall, and its thickness increases going down the flow. This corresponds to undeveloped flow in the channel. The velocity profiles in this case are S-shaped, with a point of inflection in the mixing zone.

With vigorous injection (Fig. 4b), the mixing zone is moved away from the wall at nearly the beginning of injection and a region with a nearly 100% concentration of the injected gas, with a cross section considerably exceeding that of the mixing zone, is formed directly at the wall. It is apparent from the interferograms that, beginning with a certain distance from the beginning of injection, the thickness of this region (displacement region) and the

mixing-zone thickness are nearly constant down the flow, i.e., the flow begins to stabilize. The longitudinal velocity distribution is linear in the displacement region and the velocity gradient changes little along the channel, which agrees with the calculated results. The velocity profile is nonlinear in the mixing zone.

The measured and calculated velocity distributions for the above-described conditions are shown in Fig. 3. The solid lines represent velocity profiles calculated without allowance for the noninertial section, while the dashed lines represent profiles calculated with allowance for this section. It can be seen from Fig. 3 that the effect of the noninertial section decreases with an increase in injection rate. Comparison of the theoretical and experimental results shows that they agree satisfactorily, except for the case of very high injection rates. Here, the solution obtained in the boundary-layer theory approximation may lead to a substantial error in the initial section of the channel.

NOTATION

x, y, longitudinal and transverse coordinates; u_x, u_y, longitudinal and transverse velocity components; p, pressure; ρ, density; ν, kinematic viscosity; h, channel width; U, mean velocity; U_0, mean velocity at the inlet section; V, injection rate; $\mathrm{Re}_V = Vh/\nu$, Reynolds number determined from injection rate; $\beta = \int_0^h u_x^2 dy/hU^2$, momentum flux coefficient; $\bar{x} = x\nu/U_0h^2$, $\bar{y} = y/h$, $\bar{u}_x = u_x/U_0$, $\bar{u}_y = u_yh/\nu$, $\bar{p} = p/\rho U_0^2$, $\bar{U} = U/U_0$, dimensionless variables.

LITERATURE CITED

1. A. S. Berman, "Laminar flow in channels with porous walls," J. Appl. Phys., 24, No. 9, 1232-1235 (1953).
2. R. M. Terril, "Laminar flow in a uniformly porous channel," Aeronaut. J., 15, No. 3, 299-310 (1964).
3. R. M. Terril and G. M. Shrestha, "Laminar flow through parallel and uniformly porous walls of different permeability," Z. Angew. Math. Phys., 1, No. 4, 470-482 (1965).
4. G. M. Shrestha and R. M. Terrill, "Laminar flow with large injection through parallel and uniformly porous walls of different permeability," Q. J. Mech. Appl. Math., 21, No. 4, 413-432 (1968).
5. Debruge and Hain, "Solution of a problem on heat exchange in a channel with a porous wall with application to turbine vane cooling," Heat Transfer, Ser. C, 94, No. 4, 54-60 (1972).
6. V. N. Varapaev, "Flow of a viscous fluid in the initial section of a plane channel with porous walls," Izv. Akad. Nauk SSSR, Mekh. Zhidk. Gaza, No. 4, 178-181 (1969).
7. Dofti and Perkins Jr., "Length of the hydrodynamic flow stabilization section between parallel porous plates," Appl. Mech., Ser. E, 37, No. 2, 294-296 (1970).
8. V. I. Alimpiev, S. V. Kalinina, and P. P. Lugovskii, "Study of the hydrodynamics of flow of a single-phase medium in narrow channels with injection," in: Turbulent Boundary Layer with Complex Boundary Conditions [in Russian], Inst. Teplofiz., Novosibirsk (1977), pp. 73-82.
9. G. Schlichting, Boundary Layer Theory, McGraw-Hill (1966).
10. V. M. Eroshenko, M. M. Morozov, and V. P. Motulevich, "Gasdynamic unit with an IT-14 interferometer," in: Physical Gas Dynamics [in Russian], Izd. Akad. Nauk SSSR, Moscow (1961), pp. 51-59.